

# Communication Scheduling as a First-Class Citizen in Distributed Machine Learning Systems

Sayed Hadi Hashemi, Sangeetha Abdu Jyothi, Roy H. Campbell  
*University of Illinois at Urbana-Champaign*

## Abstract

State-of-the-art machine learning systems rely on graph-based models, with the distributed training of these models being the norm in AI-powered production pipelines. The performance of these communication-heavy systems depends on the effective overlap of communication and computation. While the overlap challenge has been addressed in systems with simpler model representations, it remains an open problem in graph-based models.

In this work, we develop a system for communication scheduling which realizes near-optimal overlap of communication and computation in graph-based models. Our system is implemented over TensorFlow and requires no changes in the model or developer inputs. Our system improves the throughput by up to 82% in inference and 20% in training, while also reducing straggler effect by up to  $2.8\times$ . A part of our implementation is already merged with TensorFlow codebase; the rest is publicly available.

## 1 Introduction

The growth of artificial intelligence in the past decade has been fuelled by the flexibility of development offered by machine learning frameworks, availability of rich data, and readily accessible distributed high-performance computing. Graph-based machine learning models [1, 7, 29] provide the much-needed flexibility in state-of-the-art systems by decoupling the complexity of designing sophisticated models and their machine instruction-level optimization for execution. This decoupling allows developers to implement new ideas once, and efficiently run them across a wide variety of underlying hardware configurations. The computational cost of training these models has long outgrown the capabilities of a single high-end machine, leading to distributed training being the norm in a typical AI pipeline.

Training a machine learning model is an iterative job

which may take days to weeks. Iterations are computationally identical, each iteration typically lasting milliseconds to seconds. At the end of each iteration, servers have to exchange a relatively large amount of data over a communication channel. This communication overhead has a substantial impact on throughput of the system and also limits its scalability [31, 3].

There have been attempts to reduce the overhead of communication by decreasing the amount of data transferred over the network [3, 34, 38, 33, 10, 18, 17, 9, 4, 2] or by increasing the computation time per iteration [17, 9, 21, 36]. Another technique is to improve the overlap of communication and computation through better scheduling. The overlap approach has been studied in systems with layer-by-layer model representation [5, 12, 38] where finding the optimal order of execution is trivial [11], but is still an open problem in graph-based machine learning models.

In models with graphical dependencies, it is non-trivial to find the optimal schedule which maximizes the overlap between computation and communication. The schedule of data transfers in current systems is determined arbitrarily during execution without considering the impact on the overlap. This approach has two performance implications. First, the iteration time suffers significantly due to sub-optimal overlap. Second, even in the same iteration, multiple servers might follow different schedules of data transfers, leading to stragglers during synchronized training.

In this work, we devise a systematic methodology for deriving near-optimal schedules through critical path analysis for maximal overlap of computation and communication in graph-based models. We also develop a lightweight resource-level enforcement mechanism on a graph-based distributed machine learning system, TensorFlow [1]. Our method achieves substantial performance improvement while requiring no changes in the model or developer inputs.

In this work, we make the following contributions:

- We identify an opportunity for improving performance in state-of-the-art distributed machine learning systems through finer-grained resource-aware scheduling (§2).
- We define a metric to quantify the scheduling efficiency of a given execution (§3).
- We propose two heuristics, TAO and TIO, for near-optimal scheduling of computation and communication in Model Replica with Parameter Server, a commonly used distribution pattern in machine learning.
- We implement our system over TensorFlow (§5). The code is publicly available.
- We extensively evaluate the performance of our system and show that throughput can be improved by up to 82% with realistic workloads (§6).

## 2 Background and Motivation

In this section, we give a brief overview of distributed execution of graph-based models and shed light on its shortcomings. Next, we motivate our choice of Model-Replica as the representative model for tackling these issues and lay out the roadmap for our proposal.

### 2.1 Distributed Execution

Distributed execution (DE) of a model involves two stages: partitioning and execution. In partitioning, the graph associated with the model is transformed into components, each allotted to a single device. In the execution phase, the assigned component is executed on each of the devices.

**Device:** A device is a system element which is capable of executing a partitioned model and communicating with other devices. A GPU, a machine, a container, or a virtual machine may be considered as a device. A device consists of multiple resources: (a) *A computational resource* which executes the ops in the graph. (e.g., CPU, TPU, GPU, FPGA), and (b) *One or more communication channels (C)* which is responsible for inter-device transfers. (e.g. network, PCI-E). We only consider the network bandwidth at the device, and not in the inter-connect (such as bandwidth at core switches). The number of available communication channels depends on the underlying communication medium and RPC framework (e.g., gRPC, MPI, CUDA). Separate channels can handle requests independently, in parallel.

**Model:** The input model is a Directed Acyclic Graph (DAG) of vertices as predefined operations (ops) and edges as their data/control dependencies. A typical ML training job runs the DAG iteratively with the ultimate goal of updating special variables called parameters.

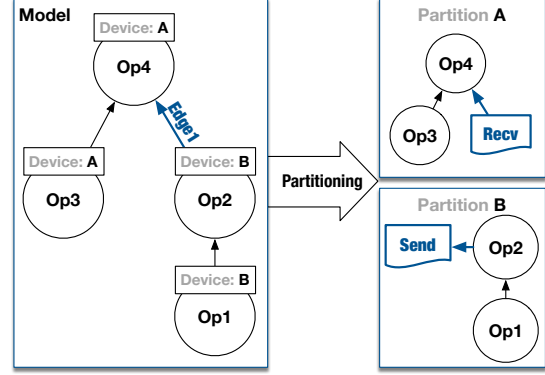


Figure 1: Example of Partitioning. The input model on the left consists of ops (represented as circles) and their associated device (represented as rectangles). On the right is the result of partitioning. In this example the cross partition edge, edge 1, is replaced by a pair of communication nodes: send, recv.

In a multi-device environment, each op in the DAG is explicitly assigned to a device. The assignment is done either manually by the model developer, or automatically through a pattern such as model-replica (more in §2.3).

**Partitioned Model:** A model is divided into components, with ops associated with a device belonging to the same partition. If two connected vertices are on different devices, the connecting edge is replaced by send and recv ops, connected to the source and destination vertices respectively. Figure 1 shows an example with 4 ops being partitioned across two devices (A and B).

**Execution:** Each device executes the partitioned graph assigned to it. The device chooses an op to execute from the list of ready-to-execute ops, i.e., ops without any outstanding dependencies. More than one op may be selected to execute at a time through multiple threads

This list also includes communication ops. When a communication op is selected for execution, it is said to be *activated*. When both peers of a communication pair are activated, the transfer is sent to the underlying RPC framework (e.g., gRPC, MPI) which follows the sequence in Figure 6 discussed in detail in §5.1.

### 2.2 Challenge in Distributed Execution

Execution of ops in DE is guaranteed to be topologically correct as specified by the DAG. However, multiple such orders are possible within the same DAG, any of which may be executed in practice.

When running on a single device, we have only one partitioned model with no communication ops, preventing any network transfer blocking on computation. However, when running on multiple devices, network may block computation depending on dependencies and the

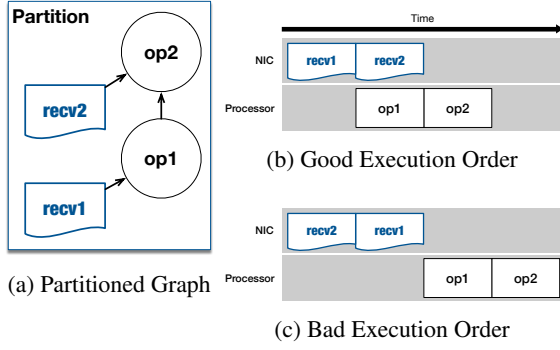


Figure 2: Impact of multi-resource operation ordering on performance

order of transfers. Hence, the computational capacity may not be fully utilized, resulting in sub-optimal performance. In addition, variation in iteration time across multiple devices can lead to straggling effect.

We illustrate the significance of ordering with a simple example. Figure 2a shows a partitioned graph which has two communication ops ( $recv_1, recv_2$ ) and two computation ops ( $op_1, op_2$ ) assigned to a device in a multi-device environment. While both  $r_1 \rightarrow r_2 \rightarrow o_1 \rightarrow o_2$  and  $r_2 \rightarrow r_1 \rightarrow o_1 \rightarrow o_2$  are valid orders topologically, as shown in figures 2b and 2c, the latter has a bad step time. This is because the good execution follows the correct use of topological order and transfer overlap.

## 2.3 Model-Replica

Many large-scale machine learning jobs in practice are distributed using Model-Replica (MR) pattern [9, 17, 13]. In MR, a base model is replicated on several devices (also known as workers) and the input data is partitioned among them. The workers collectively update a persistent collection of parameters. Therefore, during training, MR requires updates from workers to be aggregated.

Parameter server style is the method of choice for aggregation [13, 1, 8, 25]<sup>1</sup>. In this style, one or more special devices called Parameter Servers (PS) store the master copy of the parameters. A worker loads a fresh copy of parameters at the beginning of each iteration and sends updates back to the PS during the iteration. PS is responsible for aggregating the updates and applying changes to the master copy of the parameters. Figure 3 shows different elements in MR<sup>2</sup>: Base Model, Model, and Par-

<sup>1</sup>While other methods such as MPI style all reduce also has been used extensively for this very purpose, in this work we direct our focus on PS.

<sup>2</sup>Different systems may implement the MR differently. One major difference is to whether update a parameter as an update arrives or collect all the updates and aggregate once. In either case, our model and

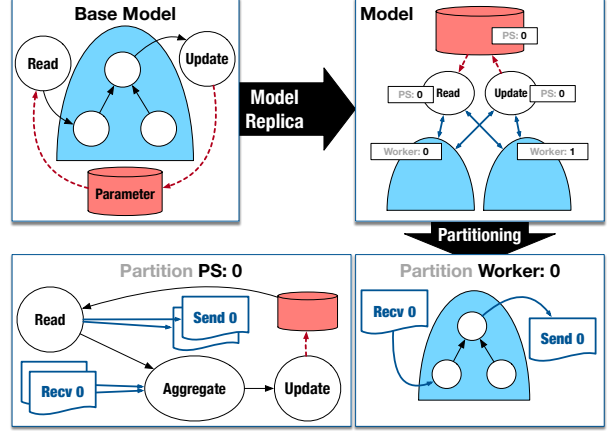


Figure 3: Distributed execution of Model-Replica with Parameter Server

tioned Graphs.

**Base Model:** The base model defines a DAG of known operations including reads and updates to a set of persistent parameters. In a typical base model DAG, all the reads are leaves (ops with no dependencies), and all the updates are roots (with no ops dependent on them). Ops in a base model are not associated with any devices. In deep learning, the DAG consists of two parts: forward pass (for inference of loss) and backward pass (for calculating gradient for a given loss).

**Model:** In model, each worker has a copy of the base model DAG. In MR with PS, all workers share a single pair of read/update ops per parameter. The read/update ops and the master copy of the parameters are split across one or more Parameter Servers (PS).

**Partitioned Graphs:** The result of partitioning is two classes of partitions: 1) the PS and 2) the worker. The PS partition is independent of the structure of the base model DAG. Parameters are located in this partition, as well as their corresponding read, update and aggregate ops. The worker partition on each worker device is similar to the base model, except each read op is replaced with a *recv* op and update op is replaced with *send* op. Additionally, no parameters are located on any worker partition.

## 2.4 Ordering in Model-Replica Systems

The optimization of the MR can be reduced to the optimization of only two partition classes, the PS and the worker.

**PS:** PS has five ops per parameter: aggregation, *send*, *recv*, read, and update. Aggregation, read and update on proposed method hold.

PS are typically lightweight. The transfers are driven by the workers as PS activates all *send* and *recv* at the beginning of each iteration. Since the load on PS is dominated by network transfers, the problem of communication-computation overlap does not arise in PS.

**Worker:** In the worker partition, all *recv* ops are leaves and *send* ops are roots. *Recv* ops can only block the initialization of a branch in the DAG, the remaining of which can proceed uninterrupted until the *send* ops at the root are reached.

Therefore, the ordering in MR can be reduced to the ordering of *recv* ops in workers.

### 3 Quantifying Ordering Efficiency

As we established the impact of ordering on performance in §2, in this section, we explore methods for quantitatively comparing the efficiency of multiple orderings. Towards this goal, we formally define the ordering problem and investigate the feasibility of finding an optimal solution. Finally, we explore metrics that are used to quantify the ordering.

The objective of this exercise is to improve performance by finding the optimal order. The optimal order is an order which leads to the minimum execution time. The inputs to this optimization problem in Model Replica are: (a) *the partitioned graph*, and characteristics of the underlying platform, in terms of (b) *communication channels* and (c) *a time oracle*.

**Partitioned Graph:** Based on the nature of ops, we add resource tags to vertices in the partitioned graph assigned to each device — computation ops to computation resource, communication ops to corresponding channels.

**Time Oracle (Time):** Another input to the optimization problem is the characteristics of the underlying platform performance in the form of a time oracle. The time oracle ( $Time(op)$ ) predicts the execution time of a given op. For computation ops, this indicates the elapsed time on a computation resource. For communication ops, this represents the transfer time on the communication medium. We compute the time assuming that the resource is dedicated to the op under consideration<sup>3</sup>

**Order:** Ops in the DAG have to run in topological order. We want to limit the execution path to take only a subset of this valid set of orders. We achieve this with priority numbers.

**Priority:** Priority number is a real number assigned to an op in the partitioned graph. An op may not be assigned a priority if it need not be ordered. Multiple ops

<sup>3</sup>Implicitly we make an assumption that  $Time(op_1) + Time(op_2) = Time(op_1 + op_2)$ . While this is not the case in general, in the domain of our experiments, we notice that the error is negligible.

may be assigned the same priority if they can run in any order with respect to each other.

When the execution proceeds as described in §2.1, the order is enforced in the following manner. When a resource needs to select a new item from the ready-to-execute queue, it randomly chooses from among the ops with the lowest order number and ops without any order number. This model of execution ensures total ordering at the resource level. It is worth noting that priority only specifies relative order among candidate ops in the ready-to-execute queue, and the resulting order will still respect the topological order.

**Makespan:** With a partitioned graph, list of resources on each device, the time oracle, and a given order, we calculate the total length of the schedule, also defined as makespan. This terminology is borrowed from job shop scheduling.

The problem of finding the optimal order in an MR model can be mapped to finding the minimum makespan in a job shop problem with dependencies (flowshop in [14]), where machines are resources, tasks are ops, task dependencies are given by the DAG, and given tasks are already assigned to the machines. The solution to this problem is known to be NP-Hard [14], therefore we propose an approximate solution as a heuristic algorithm in §4. Note that we focus on prioritizing ops on individual resources within a single device, given an assignment of ops on devices. The widely-studied multi-resource/multi-processor scheduling is orthogonal to our problem and deals with assigning tasks to individual components, but does not consider relative priorities between them<sup>4</sup>.

#### 3.1 Ordering Efficiency Metric

We define a metric, Ordering Efficiency ( $E(G, Time, makespan)$ ), to measure the effect of ordering and contain variation in makespan from other sources. This metric is used to evaluate the quality of our heuristics in the absence of a polynomial solution to this NP-hard problem.

To define this more formally, we introduce upper and lower boundaries of makespan with respect to ordering. These bounds ignore the dependencies in the DAG, and hence may not be achievable.

The worst makespan (the longest) is computed by assuming only one resource is utilized at any given moment during the execution, i.e., the ops are executed sequentially. In this case, the makespan is:

$$\overline{Makespan}(G, Time) = \sum_{op \in G} Time(op) \quad (1)$$

<sup>4</sup>It should be noted that assigning devices using multi-resource scheduling is still an open problem in distributed machine learning system. It is beyond the scope of this paper.

The lower bound of the makespan is computed by assuming all the resources are always utilized (without any restrictions imposed by the DAG). The makespan in this case is:

$$\underline{Makespan}(G, Time) = \max_{r \in R} \sum_{op \in G_r} Time(op) \quad (2)$$

where  $G_r$  refer to all ops assigned to the resource  $r$ .

For a given iteration, we measure runtime of each op ( $Time(op)$ ) as well as the makespan of that iteration ( $t$ ) and then calculate the bounds on makespan. We define Ordering Efficiency<sup>5</sup> as follows:

$$E(G, Time, t) = \frac{\overline{Makespan}(G, Time) - t}{\overline{Makespan}(G, Time) - \underline{Makespan}(G, Time)} \quad (3)$$

$E = 1$  indicates a perfect ordering, and  $E = 0$  means the worst ordering.

Next, we define *Speedup*,  $S(G, Time)$ , as the maximum theoretical performance speedup possible with the best ordering relative to the worst ordering:

$$S(G, Time) = \frac{\overline{Makespan}(G, Time) - \underline{Makespan}(G, Time)}{\underline{Makespan}(G, Time)} \quad (4)$$

$S = 0$  indicates no benefit from ordering, and for example  $S = 1$  means double the throughput. Generally, if one resource on a device has significantly higher load than others, then better ordering will have less effect on the makespan since we are restricted by the bottleneck. In practice,  $S$  increases as the number of workers increases until the communication bottleneck is hit [31, 3].

## 4 Proposed Solution

In this section, we present two heuristics to approximate the optimal ordering of *recv* ops in a reference worker partition (§2.4). The intuition in our heuristics is to prioritize transfers that speeds up the critical path in the DAG. The heuristics are:

**Timing-Aware Ordering (TAO):** In this algorithm, we rely on time oracle for individual operations and dependencies among vertices to prioritize transfers that maximize the computation/communication overlap.

**Timing-Independent Ordering (TIO):** In TIO, we ignore the time for computation operations and assign priorities based only on vertex dependencies in the DAG; higher priorities are given to transfers which are least blocking on computation.

<sup>5</sup>This metric is an update to "Scheduling Efficiency" metric in original job shop problem

### 4.1 Op properties

Before delving into the algorithms, we define new properties associated with ops, given a partitioned graph ( $G$ ), a time oracle ( $Time$ ), available channels on a device for connections to multiple PSs or multiple connections to a PS ( $C$ ) and a set of outstanding *recv* ops ( $R$ ). We assume that *recv* ops not in  $R$  have their corresponding transfers completed. These properties are updated using the algorithm 1.

**Communication Dependency (op.dep):** We define communication dependency as the set of *recv* ops that the op is directly or transitively dependent on ( $op.dep$ ). For example, in figure 2a,  $op_2.dep = \{recv_1, recv_2\}$ . We extract the communication dependencies using a depth-first post-fix graph traversal on the DAG.

---

#### Algorithm 1: Property Update Algorithm

---

```
// Update properties for the given the
// set of outstanding read ops R
1 Function UpdateProperties( $G, Time, R$ ):
2   foreach  $op \in G$  do
3      $op.M \leftarrow \sum_{r \in op.dep \cap R} Time(r)$ ;
4   end
5   foreach  $op \in R$  do
6      $op.P \leftarrow 0$ ;
7      $op.M^+ \leftarrow +\infty$ ;
8   end
9   foreach  $op \in G - R$  do
10     $D \leftarrow op.dep \cap R$ ;
11    if  $|D| = 1$  then
12       $\forall r \in D : r.P \leftarrow r.P + Time(op)$ ;
13    end
14    if  $|D| > 1$  then
15       $\forall r \in D : r.M^+ \leftarrow \min\{r.M^+, op.M\}$ ;
16    end
17  end
18 end
```

---

**Communication Time (Op.M):** For a *recv* op, this is the time required to complete its corresponding transfer, given by  $Time(recvOp)$ . For other ops, this is the total time to complete all outstanding dependent transfers, given by  $\sum_{r \in op.dep \cap R} Time(r)$ . For example, in Figure 2a,  $op_1.M = Time(recv_1)$  and  $op_2.M = Time(recv_1) + Time(recv_2)$ . In a case of multiple channels this property is computed independently for each channel and the max time is chosen. For simplicity, we assume a single channel for the rest of this section. For **recv ops**, we define two additional properties.

**Directly-Dependent Compute Load (recvOp.P):** This property represents the computational benefit of com-

pleting a *recv* op. More specifically, it is the total  $Time(op)$  for all ops that can be activated only by completing this *recvOp*, but not without it. These ops are those whose communication dependencies contain only this outstanding *recvOp* (it is admissible to have communication dependencies on other completed *recv* operations). For example, in Figure 2a,  $recv_1.P = Time(op_1)$  and  $recv_2.P = 0$  since no op can execute with completion of only *recv*<sub>2</sub>.

**Impending Communication Load ( $recvOp.M^+$ ):** This property helps us to identify candidate *recv* ops to be activated, given the current *recv* is completed. In more detail, it is the minimum communication cost to activate a computation op which has multiple *recv* dependencies including the one under consideration. For example, in Figure 2a,  $read_1.M^+ = read_2.M^+ = Cost(read_1) + Cost(read_2)$ . Please note that  $recvOp.M^+$  includes the communication time of that *recvOp*.

## 4.2 Timing-Aware Ordering (TAO)

The goal of this algorithm is to prioritize those transfers which reduce the blocking of computation, i.e., speeding up transfers on the critical path. To achieve this goal, the algorithm focuses on two cases. First, it considers the opportunity for overlapping communication and computation. Second, in the case of equal overlap or absence of it, it looks at the impending transfers to choose one which eliminates the computation block sooner.

To better describe the logic, we begin with an example for each case.

**Case 1:** In Figure 4a, when deciding between two read ops, *A* and *B*, *A* should precede *B* iff:

$$\begin{aligned} A < B &\iff Makespan(A \rightarrow B) < Makespan(B \rightarrow A) \\ &\iff M_A + \max\{P_A, M_B\} + P_B < M_B + \max\{P_B, M_A\} + P_A \\ &\iff M_A + P_A + M_B - \min\{P_A, M_B\} + P_B < \\ &\quad M_B + P_B + M_A - \min\{P_B, M_A\} + P_A \\ &\iff \min\{P_B, M_A\} < \min\{P_A, M_B\} \end{aligned}$$

Therefore:

$$A < B \rightarrow \min\{P_B, M_A\} < \min\{P_A, M_B\} \quad (5)$$

**Case 2:** In Figure 4, when all *recv* ops are outstanding, their *P* is 0, making them equivalent under the comparison in Equation 5. Obviously, *recv<sub>A</sub>* and *recv<sub>B</sub>* should precede other *recv*s. Hence, we use  $M^+$  to break the ties:  $recv_A.M^+ = recv_B.M^+ = Time(recv_A) + Time(recv_B) < recv_C.M^+ < recv_D.M^+$ .

**Comparator:** We combine results from the two cases to make a comparator that extends to multiple read ops.

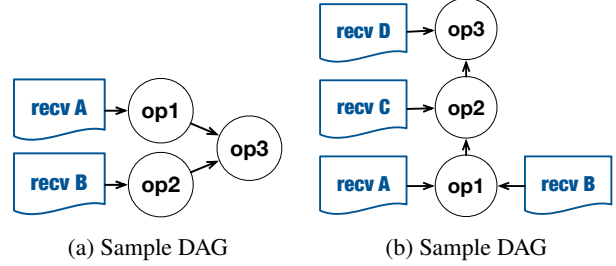


Figure 4: Sample DAG

This is an approximate induction, which may not be correct in general. The result is the *Comparator* function in algorithm 2. It is easy to prove that this function is transitive and can be used for partial ordering.

The ordering algorithm takes a partition graph on a worker, calculates the communication dependencies, then while there is an outstanding *recv* op, it updates properties, finds the smallest *recv* op with respect to the comparator and then removes the *recv* from the outstanding set and assign it a higher priority relative to others.

---

### Algorithm 2: Timing-Aware Ordering (TAO)

---

```
// Compare two given recv ops
1 Function Comparator(OpA, OpB): Bool
2   A  $\leftarrow \min(P_A, M_B)$ ;
3   B  $\leftarrow \min(P_B, M_A)$ ;
4   if A  $\neq$  B then
5     return A < B
6   else
7     return  $M_A^+ < M_B^+$ 
8   end
9 end
10 Function TAO(G, Time)
11   FindDependencies(G);
12   R  $\leftarrow \{op \mid \forall op \text{ in } G, op \text{ is } recv\}$ ;
13   count  $\leftarrow 0$ ;
14   while R is not empty do
15     UpdateProperties(G, R, Time);
16     Find the minimum op from R wrt
       Comparator;
17     Remove op from R;
18     op.priority  $\leftarrow$  count;
19     count  $\leftarrow$  count + 1;
20   end
21 end
```

---

## 4.3 Timing-Independent Ordering (TIO)

TAO is dependent on an accurate time estimate from the oracle. However, this may not be feasible in practice due

**Algorithm 3:** Timing-Independent Ordering (TIO)

---

```

1 Function TIO(G)
2   FindDependencies(G) ;
3   UpdateProperties(G, R, Time = {Computation: 0,
    Communication: 1});
4    $\forall op \text{ in } G, \text{ if } op \text{ is } recv : op.order \leftarrow op.M^+$ ;
5 end

```

---

to several reasons. First, estimating the time is difficult; it is based on past execution and collecting this information on a per op-basis introduces significant overhead to the system, especially on accelerators such as GPU. Second, the runtime may vary depending on many other factors such as system level interference. Third, time estimated on one device/software stack is not transferable to others. Device-specific estimation is cumbersome.

Therefore, it is desirable to have a heuristic independent of the platform/underlying infrastructure. Ignoring this information can obviously hurt the efficiency of the heuristic. However, our intuition is that information on DAG structure alone can provide significant improvement.

To achieve this goal, we define a generic time function, simplify the comparator and further modify TAO to reduce the impact of limited information.

**General Time Oracle:** We define a simple universal time oracle as follow:

$$Time_{General}(op) = \begin{cases} 0 & \text{if } op \text{ is not } recv \\ 1 & \text{if } op \text{ is } recv \end{cases} \quad (6)$$

Using this, time oracle in TIO reduces the *Comparator* operator to a simple  $M^+$  comparator, which eliminated the need for updating properties dynamically. Next, as an optimization, we introduce partial ordering. The idea is that we relax the priority of *recv* ops with the same  $M^+$  to allow them to run in parallel, which is achieved by assigning the same priority number to them. The full algorithm is shown in Algorithm 3.

## 5 System Design

In this section, we provide a brief overview of the system design and implementation.

The system has four main components: the tracing module, the time oracle estimator, the ordering wizard, and the enforcement module (shown in Figure 5).

**Tracing Module:** This module collects runtime stats from an execution, which is later fed to the time oracle estimator.

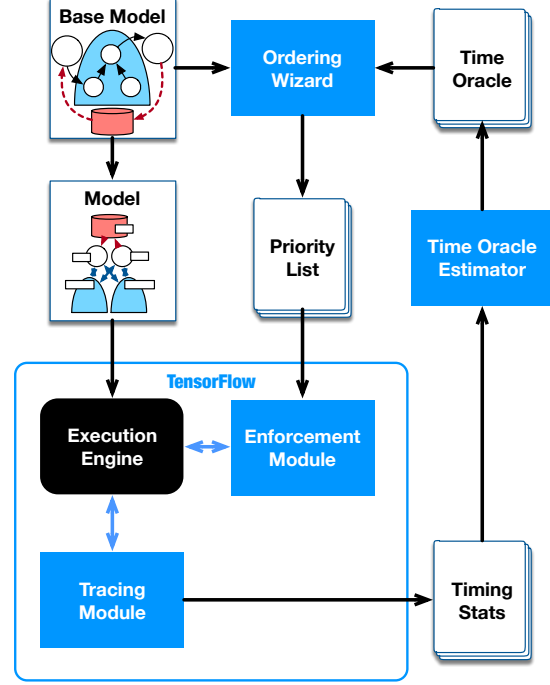


Figure 5: System Design. Components of our system are in blue sharp-edged rectangles.

**Time Oracle:** The time oracle is responsible for estimating the runtime of each op in the system based on the execution timing stats. Note that the runtime may vary depending on the platform, device characteristics, input data and even across iterations on the same hardware/software. The minimum of all measured time for a given op is chosen as the time for that op.

**Ordering Wizard:** This module is responsible for assigning priorities to *recv* ops on a single worker. The order may be computed based on TAO or TIO. In TAO, the ordering module relies on the time estimated by the time oracle. In TIO, the order is determined based on the DAG alone. The estimated priorities are sent to the enforcement module. The priority list is calculated offline before the execution; all iterations follow the same order.

**Enforcement Module:** This module takes as input the priority list computed by the ordering module and enforces this order on the network transfers per worker.

### 5.1 Implementation

We implement our system over TensorFlow<sup>6</sup>. We describe our implementation in detail.

**Time Oracle:** We use the TensorFlow internal tracer to

<sup>6</sup>top of the tree as of December 1, 2017: <https://github.com/tensorflow/tensorflow/commit/efbdc15b280374607895ab0ada467de4a0512e0c>



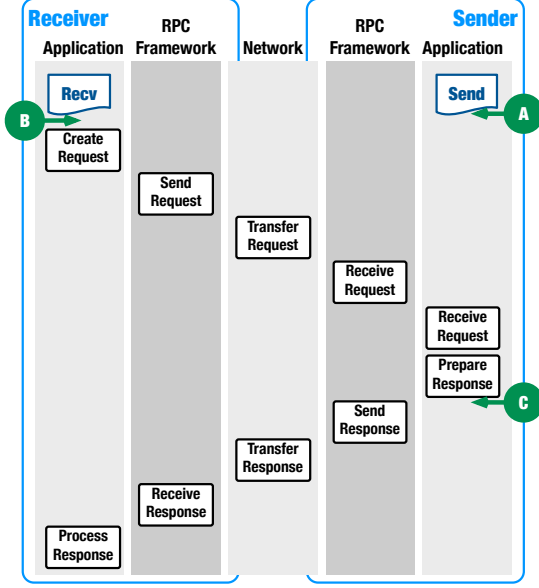


Figure 6: Life time of a network transfer.

measure the time of computation ops. We extend the capability (115 LOC C++) of this tracer to collect information on network transfer at all workers. This implementation has been already merged with TensorFlow source code<sup>7</sup>. Visualization of the performance improvement achieved with our ordering can be found at the [19].

**Ordering Wizard:** We implement TAO and TIO as offline analyzers (250 LOC in Python)<sup>8</sup>. The implementation takes time oracle and base model in the TensorFlow DAG format and generates the priority of recv ops.

**Enforcing:** The enforcement module is implemented over the gRPC submodule of TensorFlow (40LOC in C++).

gRPC provides one channel per sender-receiver pair with all transfers between the pair sent to the same queue. Only one transfer can be active at a given moment for each channel. A network transfer over gRPC in TensorFlow involves multiple stages as shown in Figure 6. When a recv op is activated at the receiver, it sends a request for transfer to the sender. If the send op is also active at the sender, the transfer may be initiated by gRPC. In this dataflow, there are three possible candidate locations for enforcing ordering — at the receiver before the request is initiated, at the sender before the send op is activated or at the sender before the transfer is sent to gRPC. Alternatively, this may also be enforced as a direct dependency in the DAG.

We implement the enforcement module at the sender

before the transfer is sent to gRPC. This choice is guided by several practical concerns. Enforcing directly on the DAG is conservative since each transfer has to wait for the completion of the previous transfer. This prevents pipelining and drastically reduces the communication throughput. Ordering the activation of recv or send ops is not sufficient since it could change throughout the data flow. For example, a larger transfer request may take longer to reach the response state on the sender side. During this interval, a smaller transfer with lower priority may catch up.

For the purpose of enforcement, the priorities are sequentially assigned to an integer in the range of  $[0, n)$ . Thus, the priority number of a transfer represents the number of transfers that have to complete before it. The sender (PS server) maintains a counter for each worker per iteration which is incremented when a corresponding transfer is handed to the gRPC. Before a transfer is handed to the gRPC, it is blocked until the corresponding counter reaches the normalized priority number.

During experiments, we notice that gRPC may not always process transfers in the order they are queued. This affects the performance of our ordering in some cases. However, the number of such occurrences at the gRPC level are very few. In Inception model (one of the tested models), this error was 0.4% in TAO and 0.5% in TIO.

## 6 Results

In this section, we evaluate our system under a wide range of inputs and system parameters to answer the following questions:

- What is the goodness-of-fit for our metric, ordering efficiency?
- How well do the proposed heuristics perform in terms of performance consistency, speedup, and straggler mitigation?
- How does ordering effect change with scale out?

**Setup:** We use in-graph replication for Distributed TensorFlow [16] with synchronized training and synthetic input data. For each experiment, we choose a batch size that gives  $S(G, Time) > 0.9$ . We use a commodity cluster with a 32 Xeon processor and 1GbE network and run our experiments with one PS and four workers, each on a separate node. We believe that our results are generalizable to systems with different hardware configurations such as those with GPU or InfiniBand since our focus is on ordering of network transfers, not the performance capability of individual components.

We tested our method on well-known models, *Alexnet* [24], *InceptionV2* [32], *VGG16* [30] as well as two ex-

<sup>7</sup><https://github.com/tensorflow/tensorflow/pull/14604>

<sup>8</sup><https://github.com/xldrx/tf-comm-scheduling>



treme toy models: *Par-32* (a flat model with 32 concurrent layers, all the topological orders are the best order in this model) and *Seq-32* (a sequential model with 32 layers similar to recurrent models, only one topological order out of 32! is the best order.)

We use Stochastic Gradient Descent (SGD) as optimizer for training base models. However, since the ratio of forward pass time and backward pass time varies extremely depending on the optimizer and the underlying platform, we report results for both forward pass and forward pass + backward pass <sup>9</sup>.

Based on collected op runtimes (§3), we also report the simulated result of two extreme ordering mechanisms: the *Theoretical Best* and *Theoretical Worst* indicate the expected results if all workers could achieve the lowest ( $E = 1$ ) and the highest ( $E = 0$ ) makespan respectively.

Next, we compare the performance metrics across various heuristics. Specifically, we evaluate throughput, ordering efficiency, and prevalence of stragglers (slow workers that force others to wait, thereby increasing the iteration time).

## 6.1 Throughput

In Figures 9a and 9d, we compare the throughput of forward pass and forward pass + gradient descent respectively. TAO and TIO offer significant speedup compared to the baseline (no ordering). Performance of TIO is comparable to that of TAO indicating that we can achieve improved performance without relying on runtime statistics in current models. The benefits are more significant in the forward pass due to substantial dependency between computation and communication. In most cases, TIO and TAO achieve near-*Theoretical best* throughput.

## 6.2 Ordering Efficiency

To validate the ordering efficiency metric, we run the forward pass of InceptionV2 1000 times each with and without the ordering algorithm (TAO). Ordering efficiency can predict step time accurately, with a high  $R^2$  score of 0.98, as seen in Figure 7. We also observe that in the absence of enforced ordering, the step time and ordering efficiency have a large variance. With ordering, the step time is reduced and the variance is minimal. Moreover, most runs have an ordering efficiency approaching 1, indicating near-optimal ordering in TAO.

In Figures 9b and 9e, we observe that ordering efficiency of the baseline is much worse than that of both the ordering algorithms, TAO and TIO. In these figures, Theoretical best (always at 1) and Theoretical worst (always at 0) are omitted. The baseline may not always suffer

<sup>9</sup>In our experience, even a simple compiler flag could change this ratio by an order of magnitude.

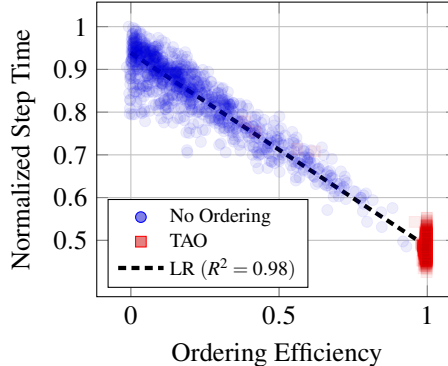


Figure 7: Regression test of Ordering Efficiency and Normalized Step Time. Sampled from Inceptionv2 forward pass.

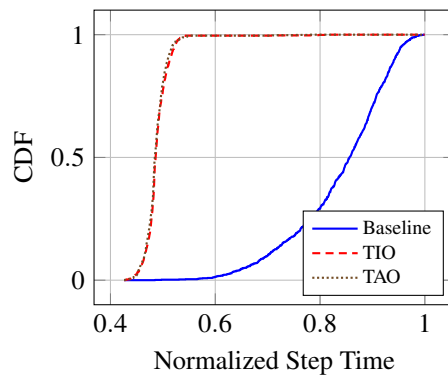


Figure 8: Step Time Comparison across Ordering Mechanisms

from the worst-case ordering. As we have already seen in Figure 7, the variance is large in this scenario. In some workloads, namely InceptionV2 and VGG16, the ordering algorithms achieve near-perfect ordering efficiency.

## 6.3 Performance Consistency

In Figure 8, we compare the consistency in performance obtained with ordering (both TAO and TIO) as well as in the absence of enforced ordering on forward pass of InceptionV2 with 1000 runs. We see that both TAO and TIO have consistent performance, denoted by a sharp curve in the CDF. The baseline (no ordering), on the other hand, has a large variance. For comparison, 95<sup>th</sup> percentile of normalized step time in the baseline, TIO, and TAO are respectively 0.63403, 0.99819, and 0.99825. Performance of TIO is only marginally worse compared to TAO. This indicates that, for current models, DAG-level information is sufficient for obtaining a near-optimal ordering. However, we expect the gap between TIO and TAO to increase as complexity of models increases.

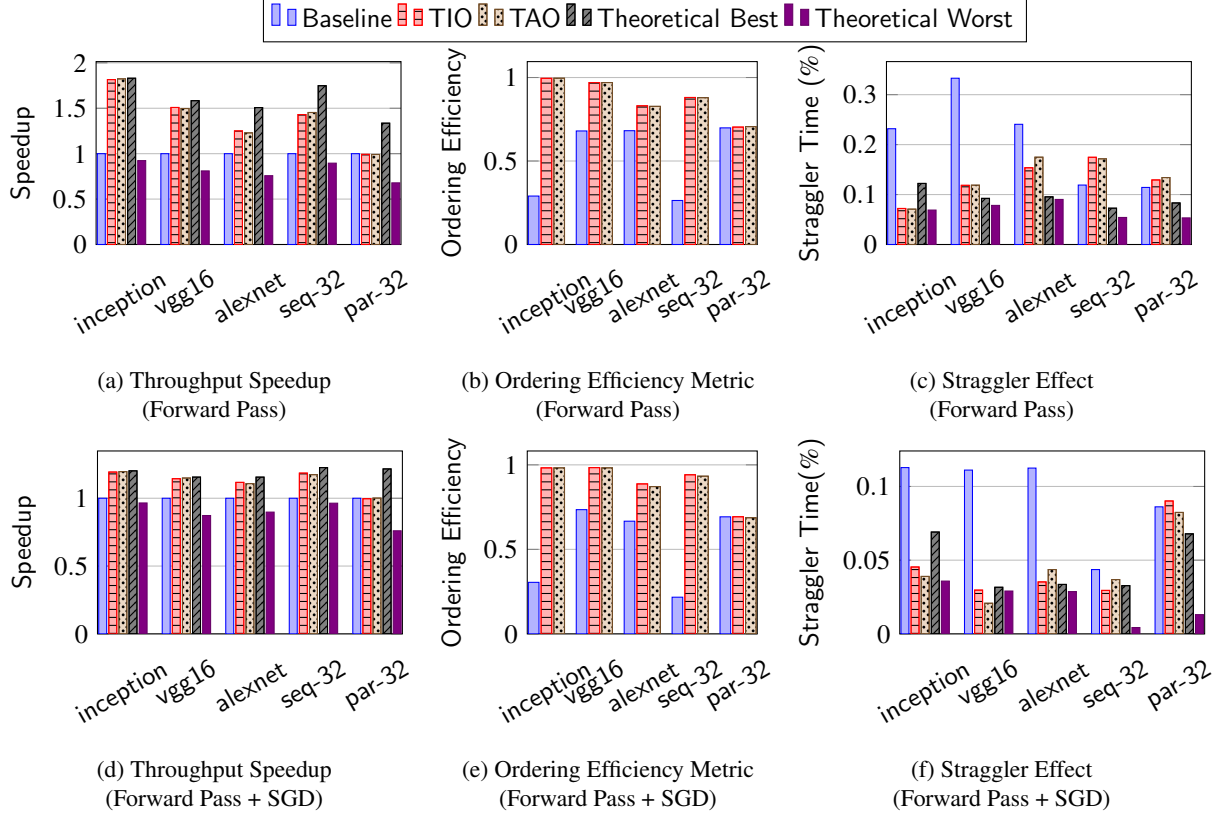


Figure 9: Performance metrics with synchronized training on 1-PS, 4-worker cluster. Baseline indicates training job without enforced network transfer ordering (vanilla TensorFlow). Based on collected op runtimes (§3), *Theoretical Best* and *Theoretical Worst* indicate the expected results if all workers could achieve the lowest ( $E = 1$ ) and the highest ( $E = 0$ ) makespan respectively (§3.1).

**Straggler Effect:** Performance inconsistency creates straggling worker effect. It happens when, in a synchronized training, multiple workers have different makespan. As a result, all workers have to wait for the slowest one. We quantify the straggler effect as the ratio of the maximum time spent by any worker in waiting to the total iteration time. Enforcing order reduces straggler effect regardless of the quality of the chosen order.

In Figures 9c and 9f, we show the impact of stragglers. Straggler effect is caused by two factors: system-level performance variations and efficiency of ordering on individual workers. In the baseline, workers follow arbitrary ordering. Hence, a worker with a bad order forces other workers into a long wait, more than 30% of the total iteration time in some cases. The differences among TIO, TAO, Theoretical best, and Theoretical worst are negligible, with the observed variations arising from system-level variations.

Interestingly, in par-32 and seq-32, where permutation of orders does not affect makespan (all orders are best in par-32 and all orders are most likely worst in seq-32), the straggler effect remains small.

## 6.4 Impact of Scaling on Ordering

In Figure 10, we examine the impact of scaling the number of workers by comparing performance speedup under 1 worker and 4 workers. For each configuration, we plot the speedup of TAO with respect to the baseline with the same configuration. Since the step time is determined by the slowest worker, the impact of worst-case increases with the number of workers. Hence, baseline with large variance has a higher probability to hit the bad cases as the number of worker increase. Thus, benefits provided by ordering are amplified as the number of workers increases, as expected.

In summary, we have shown that (a) the order of network transfers has significant impact on system throughput with order enforcement providing up to 82% gains on inference and 20% in training, (b) ordering reduces straggler effect, irrespective of the quality chosen order (c) in current models, performance of TIO which only relies only on the DAG is comparable to that of TAO which additionally uses runtime statistics (we expect this gap to widen as model DAGs become more complicated), and

(d) impact of efficient ordering is amplified as the number of nodes in the system increases.

## 7 Related Work

Model representation in machine learning systems evolved from layer-by-layer models [22] to directed acyclic graphs [1, 7, 29], with more general graphs under consideration [37, 27]. Parameter Server has been the principal way of distributing ML applications [15]. Communication in PS began in the asynchronous mode [13, 39, 26, 8], advanced to bounded asynchronicity [25] and converged to complete synchronization [1, 6].

Overlap of communication and computation is a critical challenge in distributed ML systems as communication cost increases with scale out [31, 3]. Several solutions have been proposed to tackle this problem.

**Increasing computation time:** The fraction of computation time increases with the batch size [21]. However, this approach suffers from decreased accuracy [23] which needs additional correction mechanisms [17, 9, 36, 2].

**Decreasing communication time:** Solutions to reducing network communication have taken multiple approaches — modifying the machine learning algorithm to reduce communication cost [3, 34, 38], reducing the precision of parameter representation [33, 10, 18], changing the network primitives to collective (e.g. all reduce) [17, 9, 4, 36, 2] or broadcast [38]. These approaches are orthogonal to the scope of our work. Our solution achieves high performance without modifying the communication pattern.

**Smarter interleaving of computation and communication:** This approach is adopted by several layer-by-layer systems [5, 12, 38] where the models are sequen-

tial and obtaining the order is trivial [11]. These solutions are not applicable to current DAG-based systems explored in our paper. The inter-resource dependency considered in [12] (with GPU memory) and in [38] (with network) is constrained to layer-by-layer models. Our order extraction may be coupled with enforcement techniques in these systems to extend them to modern DAG-based models. To the best of our knowledge, this work is the first to provide a solution for smarter interleaving of communication and computation in DAG models.

It is worth noting that graph-based machine learning systems are fundamentally different from graph processing systems [28, 20, 35]. In machine learning, the graph is a representation of the process to be done on the input data and not the input to the computation as is the case with graph processing systems. As a result, graphs in ML systems are a few orders of magnitude smaller than a typical large-scale graph processing system. Iterations in ML system are identical, and network communication pattern is fixed. This may not be true for graph processing systems.

## 8 Conclusion

In this work, we elucidated the importance of communication scheduling in distributed machine learning systems. We devised a metric for quantifying the efficiency of a given ordering of data transfers and developed two heuristics for efficient ordering. Through extensive testing of these heuristics across a variety of workloads, we demonstrated that significant gains are achievable through communication scheduling. For a typical machine learning training which runs for days to weeks, 82% improvement can save significant compute power.

Our study encourages further research in network scheduling for parameter server as well as other unexplored transfer patterns such as all reduce. In future, we may also take into account additional metrics such as congestion from the network fabric for better network performance. The initial results also provide motivation for extending the scheduling to additional resources types such as memory and storage.

## 9 Acknowledgements

This material is based upon work supported by the National Science Foundation under award no. 1725729. We thank Paul Barham and Brighten Godfrey for their insightful feedback.

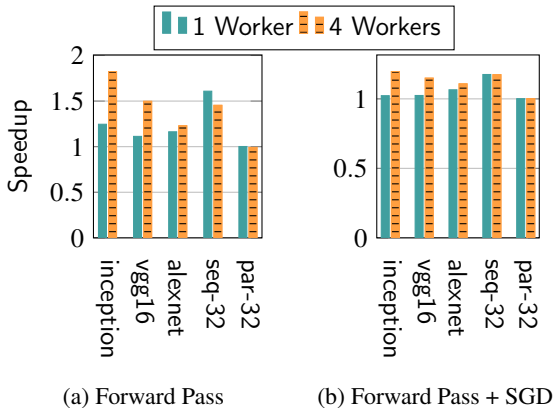


Figure 10: Comparing speedup gain of TAO with respect to the number of workers (1 vs. 4)

## References

- [1] ABADI, M., BARHAM, P., CHEN, J., CHEN, Z., DAVIS, A., DEAN, J., DEVIN, M., GHEMAWAT, S., IRVING, G., ISARD, M., ET AL. TensorFlow: A System for Large-Scale Machine Learning. In *OSDI* (2016), vol. 16, pp. 265–283.
- [2] AKIBA, T., SUZUKI, S., AND FUKUDA, K. Extremely Large Minibatch SGD: Training ResNet-50 on ImageNet in 15 Minutes. *CoRR abs/1711.04325* (2017).
- [3] ALISTARH, D., GRUBIC, D., LI, J., TOMIOKA, R., AND VOJNOVIC, M. QSGD: Communication-Efficient SGD via Gradient Quantization and Encoding. In *Advances in Neural Information Processing Systems* (2017), pp. 1707–1718.
- [4] AMODEI, D., ANUBHAI, R., BATTENBERG, E., CASE, C., CASPER, J., CATANZARO, B., CHEN, J., CHRZANOWSKI, M., COATES, A., DIAMOS, G., ELSÉN, E., ENGEL, J., FAN, L., FOGNER, C., HAN, T., HANNUN, A. Y., JUN, B., LEGRESLEY, P., LIN, L., NARANG, S., NG, A. Y., OZAIR, S., PRENGER, R., RAIMAN, J., SATHEESH, S., SEETAPUN, D., SENGUPTA, S., WANG, Y., WANG, Z., WANG, C., XIAO, B., YOGATAMA, D., ZHAN, J., AND ZHU, Z. Deep Speech 2: End-to-End Speech Recognition in English and Mandarin. *CoRR abs/1512.02595* (2015).
- [5] ARNOLD, S. An Introduction to Distributed Deep Learning. [https://seba1511.com/dist\\_blog/](https://seba1511.com/dist_blog/), 2016.
- [6] CHEN, J., PAN, X., MONGA, R., BENGIO, S., AND JOZEFOWICZ, R. Revisiting distributed synchronous SGD. *arXiv preprint arXiv:1604.00981* (2016).
- [7] CHEN, T., LI, M., LI, Y., LIN, M., WANG, N., WANG, M., XIAO, T., XU, B., ZHANG, C., AND ZHANG, Z. Mxnet: A flexible and efficient machine learning library for heterogeneous distributed systems. *arXiv preprint arXiv:1512.01274* (2015).
- [8] CHILIMBI, T. M., SUZUE, Y., APACIBLE, J., AND KALYANARAMAN, K. Project Adam: Building an Efficient and Scalable Deep Learning Training System. In *OSDI* (2014), vol. 14, pp. 571–582.
- [9] CHO, M., FINKLER, U., KUMAR, S., KUNG, D., SAXENA, V., AND SREEDHAR, D. PowerAI DDL. *arXiv preprint arXiv:1708.02188* (2017).
- [10] COURBARIAUX, M., BENGIO, Y., AND DAVID, J.-P. Binaryconnect: Training deep neural networks with binary weights during propagations. In *Advances in neural information processing systems* (2015), pp. 3123–3131.
- [11] CUI, H., TUMANOV, A., WEI, J., XU, L., DAI, W., HABERKUCHARSKY, J., HO, Q., GANGER, G. R., GIBBONS, P. B., GIBSON, G. A., ET AL. Exploiting iterative-ness for parallel ML computations. In *Proceedings of the ACM Symposium on Cloud Computing* (2014), ACM, pp. 1–14.
- [12] CUI, H., ZHANG, H., GANGER, G. R., GIBBONS, P. B., AND XING, E. P. GeePS: Scalable deep learning on distributed GPUs with a GPU-specialized parameter server. In *Proceedings of the Eleventh European Conference on Computer Systems* (2016), ACM, p. 4.
- [13] DEAN, J., CORRADO, G., MONGA, R., CHEN, K., DEVIN, M., MAO, M., SENIOR, A., TUCKER, P., YANG, K., LE, Q. V., ET AL. Large scale distributed deep networks. In *Advances in neural information processing systems* (2012), pp. 1223–1231.
- [14] GAREY, M. R., JOHNSON, D. S., AND SETHI, R. The Complexity of Flowshop and Jobshop Scheduling. *Mathematics of Operations Research* 1, 2 (1976), 117–129.
- [15] GOODFELLOW, I., BENGIO, Y., AND COURVILLE, A. *Deep Learning*. MIT Press, 2016.
- [16] GOOGLE. Distributed tensorflow. <https://www.tensorflow.org/deploy/distributed>.
- [17] GOYAL, P., DOLLÁR, P., GIRSHICK, R., NOORDHUIS, P., WESOŁOWSKI, L., KYROLA, A., TULLOCH, A., JIA, Y., AND HE, K. Accurate, Large Minibatch SGD: Training ImageNet in 1 Hour. *arXiv preprint arXiv:1706.02677* (2017).
- [18] GUPTA, S., AGRAWAL, A., GOPALAKRISHNAN, K., AND NARAYANAN, P. Deep learning with limited numerical precision. In *International Conference on Machine Learning* (2015), pp. 1737–1746.
- [19] HASHEMI, S. H. TensorFlow Runtime Tracing Metadata Visualization. <https://github.com/xldrx/tensorflow-runtime-metadata-visualization>, 2018.
- [20] HOQUE, I., AND GUPTA, I. LFGraph: Simple and fast distributed graph analytics. In *Proceedings of the First ACM SIGOPS Conference on Timely Results in Operating Systems* (2013), ACM, p. 9.
- [21] IANDOLA, F. N., MOSKEWICZ, M. W., ASHRAF, K., AND KEUTZER, K. Firecaffe: near-linear acceleration of deep neural network training on compute clusters. In *Proceedings of the IEEE Conference on Computer Vision and Pattern Recognition* (2016), pp. 2592–2600.
- [22] JIA, Y., SHELHAMER, E., DONAHUE, J., KARAYEV, S., LONG, J., GIRSHICK, R., GUADARRAMA, S., AND DARRELL, T. Caffe: Convolutional architecture for fast feature embedding. In *Proceedings of the 22nd ACM international conference on Multimedia* (2014), ACM, pp. 675–678.
- [23] KESKAR, N. S., MUDIGERE, D., NOCEDAL, J., SMELYANSKIY, M., AND TANG, P. T. P. On large-batch training for deep learning: Generalization gap and sharp minima. *arXiv preprint arXiv:1609.04836* (2016).
- [24] KRIZHEVSKY, A., SUTSKEVER, I., AND HINTON, G. E. ImageNet classification with deep convolutional neural networks. In *Advances in neural information processing systems* (2012), pp. 1097–1105.
- [25] LI, M., ANDERSEN, D. G., PARK, J. W., SMOLA, A. J., AHMED, A., JOSIFOVSKI, V., LONG, J., SHEKITA, E. J., AND SU, B.-Y. Scaling Distributed Machine Learning with the Parameter Server. In *OSDI* (2014), vol. 1, p. 3.
- [26] LI, M., ANDERSEN, D. G., SMOLA, A. J., AND YU, K. Communication efficient distributed machine learning with the parameter server. In *Advances in Neural Information Processing Systems* (2014), pp. 19–27.
- [27] LOOKS, M., HERRESHOFF, M., HUTCHINS, D., AND NORVIG, P. Deep learning with dynamic computation graphs. *arXiv preprint arXiv:1702.02181* (2017).
- [28] MALEWICZ, G., AUSTERN, M. H., BIK, A. J., DEHNERT, J. C., HORN, I., LEISER, N., AND CZAJKOWSKI, G. Pregel: a system for large-scale graph processing. In *Proceedings of the 2010 ACM SIGMOD International Conference on Management of data* (2010), ACM, pp. 135–146.
- [29] PASZKE, A., GROSS, S., CHINTALA, S., AND CHANAN, G. PyTorch: Tensors and dynamic neural networks in Python with strong GPU acceleration, 2017.
- [30] SIMONYAN, K., AND ZISSERMAN, A. Very deep convolutional networks for large-scale image recognition. *arXiv preprint arXiv:1409.1556* (2014).
- [31] SRIDHARAN, S., VAIDYANATHAN, K., KALAMKAR, D., DAS, D., SMORKALOV, M. E., SHIRYAEV, M., MUDIGERE, D., MELLEMPUDI, N., AVANCHA, S., KAUL, B., ET AL. On Scale-out Deep Learning Training for Cloud and HPC. *arXiv preprint arXiv:1801.08030* (2018).

- [32] SZEGEDY, C., VANHOUCKE, V., IOFFE, S., SHLENS, J., AND WOJNA, Z. Rethinking the inception architecture for computer vision. In *Proceedings of the IEEE Conference on Computer Vision and Pattern Recognition* (2016), pp. 2818–2826.
- [33] VANHOUCKE, V., SENIOR, A., AND MAO, M. Z. Improving the speed of neural networks on CPUs. In *Proc. Deep Learning and Unsupervised Feature Learning NIPS Workshop* (2011), vol. 1, Citeseer, p. 4.
- [34] WEN, W., XU, C., YAN, F., WU, C., WANG, Y., CHEN, Y., AND LI, H. Terngrad: Ternary gradients to reduce communication in distributed deep learning. In *Advances in Neural Information Processing Systems* (2017), pp. 1508–1518.
- [35] XIN, R. S., GONZALEZ, J. E., FRANKLIN, M. J., AND STOICA, I. Graphx: A resilient distributed graph system on spark. In *First International Workshop on Graph Data Management Experiences and Systems* (2013), ACM, p. 2.
- [36] YOU, Y., ZHANG, Z., HSIEH, C., AND DEMMEL, J. 100-epoch ImageNet Training with AlexNet in 24 Minutes. *CoRR abs/1709.05011* (2017).
- [37] ZHANG, H., XU, S., NEUBIG, G., DAI, W., HO, Q., YANG, G., AND XING, E. P. Cavs: A Vertex-centric Programming Interface for Dynamic Neural Networks. *arXiv preprint arXiv:1712.04048* (2017).
- [38] ZHANG, H., ZHENG, Z., XU, S., DAI, W., HO, Q., LIANG, X., HU, Z., WEI, J., XIE, P., AND XING, E. P. Poseidon: An Efficient Communication Architecture for Distributed Deep Learning on GPU Clusters. In *2017 USENIX Annual Technical Conference (USENIX ATC 17)* (Santa Clara, CA, 2017), USENIX Association, pp. 181–193.
- [39] ZHANG, W., GUPTA, S., LIAN, X., AND LIU, J. Staleness-aware async-sgd for distributed deep learning. *arXiv preprint arXiv:1511.05950* (2015).